

# Nanometric hollow spheres made of MSU-X-type mesoporous silica

Eric Prouzet,<sup>\*a</sup> Frédéric Cot,<sup>a</sup> Cédric Boissière,<sup>a</sup> Patricia J. Kooyman<sup>b</sup> and André Larbot<sup>a</sup>

<sup>a</sup>Institut Européen des Membranes (CNRS UMR 5635), CNRS, 1919 Route de Mende, F-34293 Montpellier Cedex 5, France. E-mail: prouzet@iemm.univ-montp2.fr

<sup>b</sup>National Centre for HREM, Delft University of Technology, Rotterdamesweg 137, 2628 AL Delft, The Netherlands

Received 10th December 2001, Accepted 15th February 2002

First published as an Advance Article on the web 8th March 2002

Submicrometric hollow spheres with mesoporous walls were prepared by applying the synthesis of MSU-X type mesoporous silica at neutral pH. The application of ultrasound in the proper power range, to a mixture of nonionic polyoxyethylene surfactant and unreacted silicon alkoxide (tetraethylorthosilicate) gives a stable emulsion where the cavitation bubbles created by the ultrasound are trapped in the solution. Further hydrolysis and condensation of the silica by the addition of sodium fluoride freezes the structure and gives a powder that exhibits a single reflection in the X-ray diffraction pattern, characteristic of a 3D-wormhole ordered porous framework. Its main feature is a large hysteresis loop in the nitrogen adsorption/desorption isotherm. This hysteresis loop corresponds to the retention of condensed nitrogen within the voids of these particles that can play the role of tanks for volatile compounds.

## Introduction

Ordered mesoporous silica, which was first reported as “low-bulk density silica”,<sup>1,2</sup> has been extensively studied by scientists from Mobil who revealed the existence of hexagonal (MCM-41) and cubic (MCM-48) porous frameworks when an assembly mechanism is induced between the long chain cationic surfactants and inorganic species.<sup>3,4</sup> Since then, the field of so-called micelle templated structures (MTS) has been widely explored and almost all kinds of surfactants have been tested.<sup>5,6</sup> Syntheses using an assembly mechanism between nonionic surfactants or triblock copolymers with silica precursors like TEOS (tetraethoxysilane  $\text{Si}(\text{OCH}_2\text{CH}_3)_4$ ) have been successful too.<sup>7</sup> These latter materials, called MSU-X silica molecular sieves, were prepared at neutral pH by using alkyl-PEO alcohols (MSU-1), alkyl-aryl PEO surfactants (MSU-2), polypropylene oxide-PEO block copolymers (MSU-3) or ethoxylated derivatives of the fatty esters of sorbitan (Tween<sup>®</sup>) (MSU-4).<sup>7-9</sup> They exhibit a porous 3D-wormhole-like structure when prepared under pH-neutral conditions but geometrically ordered frameworks were also obtained with block copolymers and syntheses under strong acidic conditions by Stucky *et al.*<sup>10,11</sup>

We demonstrated recently that accurate control of the TEOS hydrolysis rate and the silica condensation, through a two-step process, can lead to micrometer-sized homogeneous porous particles with spherical morphology.<sup>12,13</sup> In this case, the mild acidity of the aqueous solution ( $1 < \text{pH} < 4$ ) allows the TEOS to be hydrolyzed to form small silica oligomers that build a diffuse silica shell around the nonionic micelles, which leads to monodisperse spherical hybrid micelles that can exhibit diameters as large as 12 nm.<sup>14</sup> The further addition of sodium fluoride as a condensation catalyst promotes the formation of the MSU-X-type mesoporous silica. Such a synthesis leads to powders suitable for catalytic applications or separation processes such as HPLC.<sup>15</sup> However, a continuous trend of research is focused on the preparation of more complex structures: biomimetic, “bio-inspired” or hierarchically structured materials, which are now widely reported. The specific

shapes of the mesoporous silica were mediated by various structuring agents such as block copolypeptides,<sup>16</sup> nonionic block-copolymers,<sup>17,18</sup> diamines,<sup>19</sup> gemini surfactants,<sup>20</sup> quaternary ammoniums,<sup>21</sup> alkylsaccharides<sup>22</sup> or nonionic surfactants.<sup>23</sup>

Very well-ordered mesocellular silica foams were obtained by Schmidt-Winkel *et al.*<sup>18,24</sup> through the addition of 1,3,5-trimethylbenzene (TMB), an organic cosolvent (and a micelle swelling agent too) to mixtures of diluted aqueous solutions of block copolymer Pluronic P123 ( $\text{EO}_{20}\text{-PO}_{70}\text{-EO}_{20}$ ) and TEOS. An unspecified stirring led to stable emulsions that structured the reacting silica framework. Simultaneously, Bagshaw showed that rapid (750–1000 rpm) magnetic stirring of an aqueous solution of nonionic surfactant (Triton N-101 nonyl-PEO<sub>10</sub>) mixed with TEOS gave coral-like or sponge-like foams with macroscopic voids.<sup>23</sup> For this latter case, the voids were created by air bubbles resulting from the violent stirring of the soapy solution. In both previous examples, the nanoscopic structure of materials, that is the mesoporous structure as shown by nitrogen isotherms, was not disturbed by the foam processing.

However, unlike our earlier reports about the two-step synthesis of MSU-X silica at pH 1–4, where TEOS is first hydrolyzed to form small oligomers, when synthesis proceeds under neutral pH conditions ( $\text{pH} \approx 6\text{--}7$ ) with diluted reagent concentrations, the hydrophobic character of the unreacted TEOS becomes prevalent and it can play the role of a non-aqueous phase prior to its function as silica source. The drops of insoluble TEOS in water will be partially stabilized by the surfactant molecules and the structure will be further frozen by the silica framework formation, catalyzed in our process by the addition of sodium fluoride. However, the initial drops of TEOS must be broken to allow the formation of a relatively stable emulsion. Unlike magnetic stirring, which is not powerful enough, sonication (*i.e.* using ultrasound) is highly efficient for such a purpose. Besides, sonication is a tool that can drastically modify the structure of the liquid medium because the cavitation bubbles created by the ultrasound, can collapse with the liberation of a tremendous amount of

energy.<sup>25</sup> Moreover, the cavitation bubbles created by sonication in an emulsified-soap-containing medium can possibly be trapped. Therefore, depending on the liquid viscosity, an accurate control of the sonication power will lead to bubbles, trapped in the emulsion, which can act as actual templates that induce an additional hierarchical porosity. This porosity will add to the structural mesoporosity provided by the assembly between the surfactants and inorganic species. We report here that hollow spheres with mesoporous walls can be prepared by the controlled use of ultrasound as the emulsion maker.

## Experimental

$N^{\circ}$  assembly<sup>6</sup> of the MSU silicas was accomplished by using a linear commercial PEO surfactant Tergitol 15-S-12 ( $C_{15}(EO)_{12}$ ; Union Carbide, Belgium). The surfactants and the tetraethoxysilane (TEOS;  $Si(OCH_2CH_3)_4$ , Acros Organics) were used without further purification. All materials were synthesized in an open container from aqueous mixtures of TEOS, surfactant, and sodium fluoride as a mineralizer. A typical molar composition of the reaction mixture was: surfactant, 0.02; TEOS, 0.16; NaF, 0.004; and  $H_2O$ , 55.6. In a typical preparation, 1.028 g of Tergitol 15-S-12 was first dissolved in 50 mL of water. Once surfactant dissolution was complete, 1.664 g of TEOS was added dropwise under magnetic stirring, then sonication was performed in an ice-bath, with a 600 W tunable Vibracell 72412 (Biolock Scientific) ultrasound gun (probe diameter, 10 mm) along with continuous magnetic stirring. The sonicator was set at a defined potential power but the power actually transmitted to the medium depended on its composition (the effective delivered value is measured by the sonicator). We evaluated first the correspondence between the assigned power and the power effectively delivered to the system (TEOS + surfactant + water) (Fig. 1). It appeared that one cannot transfer a power higher than 100 W to this medium. In the following, we will refer to the assigned power, which was adjusted between 6 and 180 W. We ensured that roughly the same amount of energy was transferred to the solution, whatever the sonication power, by adjusting the sonication time to between 1 and 10 min (Fig. 2). Sodium fluoride (0.84 mL of a 0.238 M NaF solution) was then added in order to reach the molar ratio  $NaF:TEOS = 2\%$ . The solution thus obtained was aged under slow shaking at 35 °C for 48 h. A white colloidal suspension appeared that settled progressively. The powder was filtered, dried, and calcined in air at 200 °C for 6 h, then at 620 °C for 6 h (heating rate, 5 °C  $min^{-1}$ ). Synthesis of a “reference” compound according to the two-step process under mild acidity, was performed according to previously reported syntheses.<sup>12,26</sup> All materials were characterized by scanning electron microscopy (SEM), X-ray diffraction (XRD), nitrogen adsorption at 77 K and transmission electron microscopy (TEM). TEM was performed using a Philips

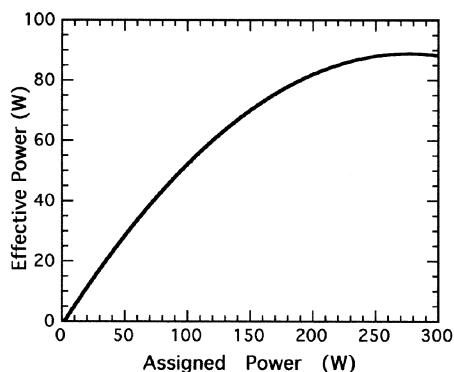


Fig. 1 Correspondence between the assigned power of the sonication gun and the effective power transmitted to the aqueous medium.

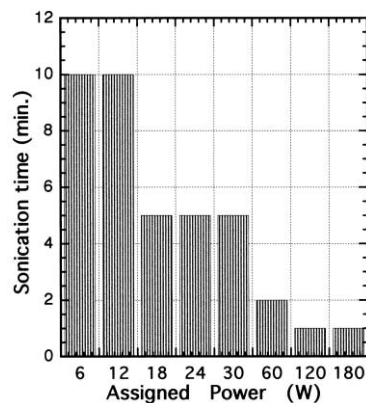
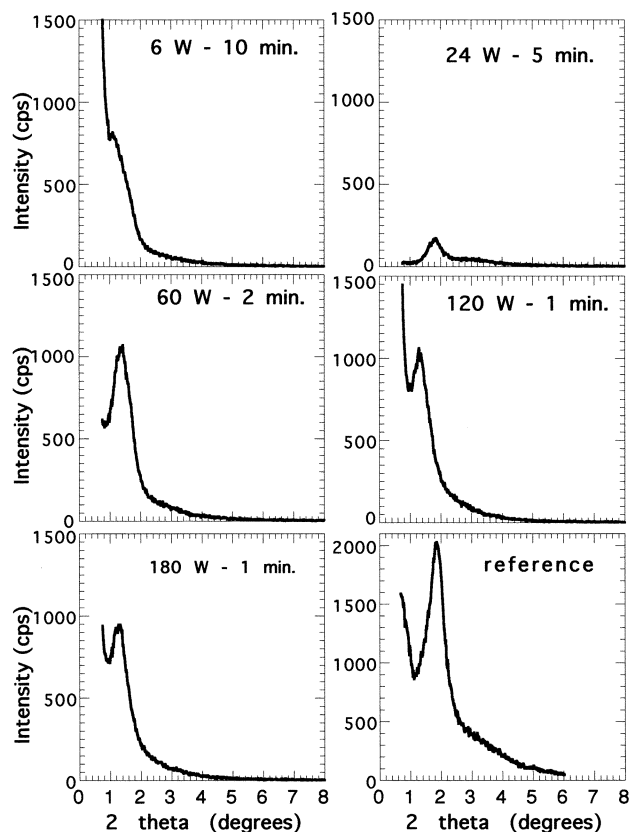


Fig. 2 Sonication time allowed for the preparation of the solutions, as a function of the assigned sonication power.

CM30/T electron microscope with a  $LaB_6$  filament as a source of electrons operated at 300 kV. Samples were mounted on a microgrid carbon polymer supported on a copper grid by placing a few droplets of a suspension of ground sample in ethanol on the grid, followed by drying under ambient conditions. SEM micrographs were obtained on a Hitachi S-5400 FEG microscope. Nitrogen adsorption isotherms were measured at 77 K on a Micromeritics 2010 Sorptometer using standard continuous procedures; the samples were first degassed at 150 °C for 15 h. The XRD patterns were recorded with a Bruker D5000 diffractometer in Bragg–Brentano reflection geometry.  $Cu-L_{3,2}$  radiation was employed that was monochromatized by a graphite single crystal in the diffracted beam. The X-ray patterns exhibit a single peak corresponding to the pore center-to-center correlation length, from which both the  $d$ -spacing and the peak broadening (FWHM) were calculated.

## Results

The XRD patterns of the materials synthesized under different conditions of sonication, are displayed in Fig. 3, along with that of the reference MSU-X silica material prepared with the two-step synthesis procedure. All materials exhibit a single diffraction line characteristic of the worm-hole structure of MSU-X-type materials.<sup>7</sup> The overall quality of the structure can be estimated from the intensity of this diffraction peak. Low sonication power (6–24 W) gives only poorly structured materials and it appears that a relatively high assigned ultrasound power (30–60 W) is required if one wants to achieve a good structure for the mesoporous framework, even if it is far worse than the structure achieved by the two-step synthesis (to compare with the “reference” in Fig. 3). SEM also reveals that the shape and size of the particles are different. Whereas particles of the reference sample are spherical, with a micrometric size range (Fig. 4c),<sup>12,26</sup> the powders prepared under ultrasound consist of aggregates of submicrometric particles (Fig. 4a and b) for the whole range of sonication power. However, the main difference is revealed by the nitrogen adsorption isotherms. The isotherm of the sample prepared according to the two-step synthesis (see “reference” in Fig. 5), does not exhibit any hysteresis, characteristic of pore necking, nor does the adsorption increase at high relative pressure, characteristic of a textural porosity. Unlike this sample, the nitrogen adsorption/desorption isotherm of the material prepared under neutral pH and with an ultrasound power of 30 W, exhibits a small increase in the 0.8–1.0  $P/P_0$  range of the adsorption curve, which can be explained by intergranular porosity between small particles, as displayed in the SEM pictures. A similar behavior is observed with the sample prepared using a 6 W ultrasound power, but an additional hysteresis, between the adsorption and the



**Fig. 3** X-ray patterns of samples prepared with different assigned sonication powers, compared with a reference of MSU-1 silica prepared according to the two-step process.

desorption branches, is observed. The steep step in the desorption curve cannot be correlated with any pore size because it is due to catastrophic desorption of nitrogen, at a characteristic  $P/P_0$  value of 0.43. The same features are

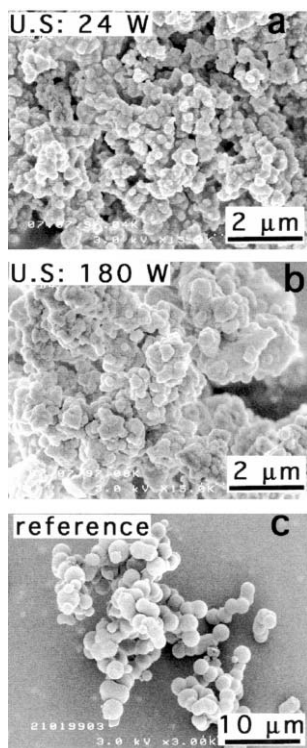


**Fig. 4** SEM images of samples prepared with 24 W and 180 W assigned power, compared with a reference of MSU-1 silica prepared according to the two-step process.

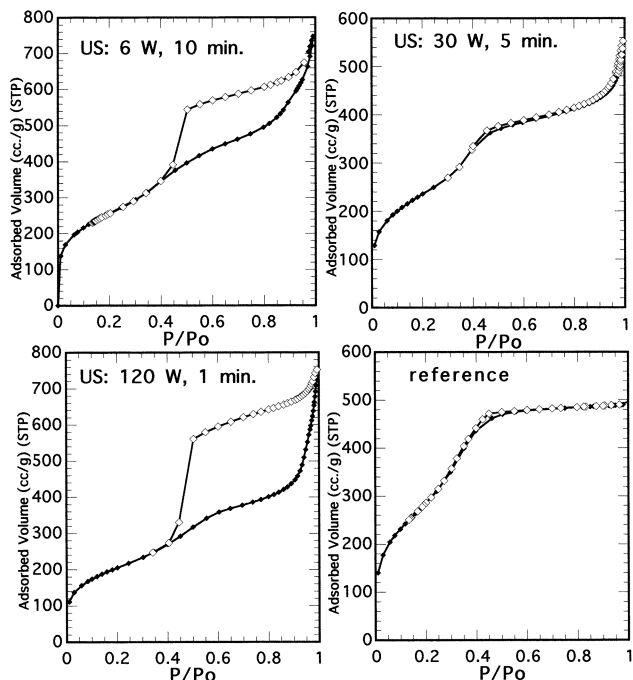


**Fig. 5** Nitrogen adsorption (◆)/desorption (◇) of samples prepared with 6 W, 30 W and 180 W assigned power, compared with a reference of MSU-1 silica prepared according to the two-step process.

observed with the sample prepared with a higher sonication power (120 W), but both (the adsorption increase and the hysteresis) are larger. Direct observations of the nanostructures of the materials by TEM (Fig. 6) provide final clues for explaining the differences observed in the nitrogen isotherms. The structure of the materials prepared with low sonication power (Fig. 6a) is heterogeneous and it looks like an aggregation of small porous particles, which can explain the origin of the textural porosity observed in the nitrogen adsorption isotherm. For the sample prepared with an intermediary power of 30 W (Fig. 6b), the porous framework appears to be homogeneous and characteristic of the 3D-wormhole porosity of MSU-X silica materials.<sup>7,26</sup> Finally, the silica prepared with a sonication power of 120 W (Fig. 6c and 6d) is made of 200–400 nm hollow spheres with mesoporous walls.

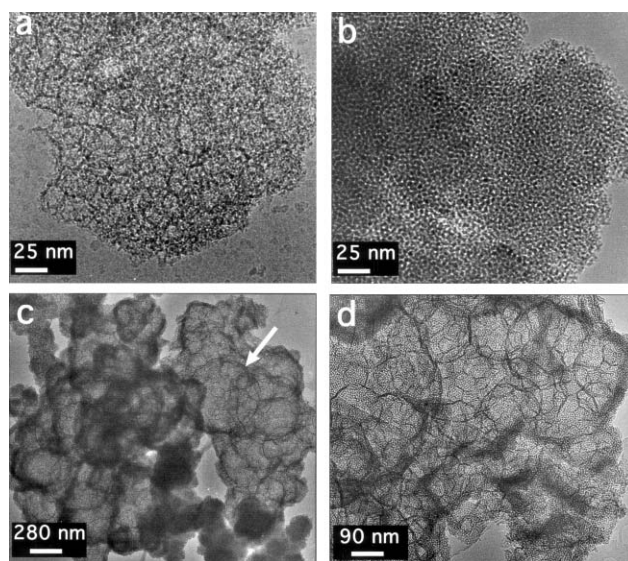


**Fig. 6** TEM images of samples prepared with 6 W (a), 30 W (b) and 120 W (c, d) assigned sonication power.

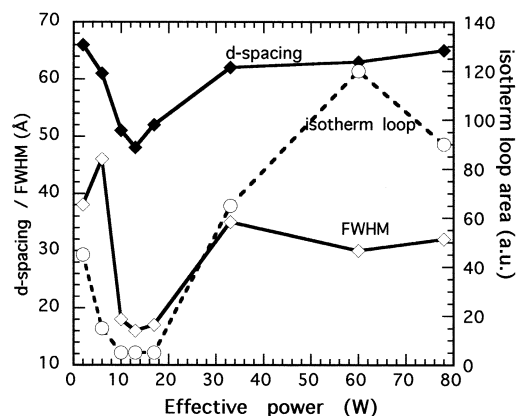


Fig. 7 Evolution of the structural parameters as a function of the effective power of sonication:  $d$ -spacing (◆) and FWHM (◇) of the diffraction line and the isotherm loop area (○)

## Discussion

When the two-step synthesis of MSU-X silica is performed at pH 2–4, it begins with an assembly mechanism between the silica oligomers prepared from the hydrolysis of TEOS or sodium silicate and the micelles of the nonionic surfactants, which leads to three-layered hybrid micelles.<sup>13,14</sup> The addition of sodium fluoride promotes the condensation of these hybrid micelles and the formation of the mesoporous silica. Unlike this process, under neutral pH conditions, TEOS cannot be hydrolyzed readily and its mixing with the aqueous solution of surfactant, under ultrasound, leads to a complex emulsion where cavitation bubbles can be trapped and template for future voids in the inorganic framework. The final structure, at different scales, will hence depend on the degree of intimacy between the hydrophilic and hydrophobic components and the gas bubbles. In order to better quantify the ordering of the materials, we plot in Fig. 7 the variation of three structural parameters, namely, (i) the  $d$ -spacing of the correlation peak, (ii) the full width at half maximum (FWHM) of this peak and (iii) an estimation of the isotherm hysteresis calculated from the difference between the desorption and the adsorption branches as a function of the effective power of sonication, considering that the total delivered energy was fairly constant (between 1.4 and 5.1 kW s). The evolution of these three parameters reveals that there are three different processes in the structuring of the material, depending on the effective applied sonication. Below 10 W, the sonication power seems to be too low to allow a good breaking of the TEOS drops and one obtains an ill-ordered heterogeneous material with a nitrogen adsorption/desorption isotherm that exhibits a small hysteresis characteristic of bottle-necked pores. A 10–20 W sonication power seems more suitable for obtaining a better ordered material; the diffraction peak broadening is smaller and one observes no loop in the nitrogen adsorption isotherm. However, one must bear in mind that it has been shown that a synthesis implying a two-step process is by far the most suitable for achieving highly ordered materials.<sup>12</sup> One may assume that in the 10–20 W range, the sonication power is powerful enough to break the TEOS drops, which allows a good mixing of components before reaction, but that it is not powerful enough to create stable gas bubbles by the cavitation process. Finally, above 40 W, the value of  $d$ -spacing remains constant, as well as the FWHM, which

reveals that the nanostructure of the material is not disturbed by the sonication at the nanometric level. Nevertheless the isotherm loop reaches tremendous values, which cannot be explained by a simple pore-necking mechanism. This behavior must be explained by a retention mechanism of the nitrogen trapped in the material. Indeed, as shown by TEM, these hollow particles with mesoporous walls, exhibit a hierarchical structure where the particles act as tanks for the nitrogen; it can penetrate within the void with an increase of the relative pressure but its desorption will occur only when a decreasing relative pressure of nitrogen reaches the desorption edge in the mesoporous walls. At this stage, a catastrophic desorption of nitrogen occurs before reaching the corresponding value for desorption from the mesoporous walls.

## References

- 1 V. Chiola, J. E. Ritsko and C. D. Vanderpool, *US Pat.*, 3 556 725, 1971.
- 2 F. D. Renzo, H. Cambon and R. Dutartre, *Microporous Mater.*, 1997, **10**, 283.
- 3 C. T. Kresge, M. E. Leonowicz, W. J. Roth, J. C. Vartuli and J. S. Beck, *Nature*, 1992, **359**, 710.
- 4 J. S. Beck, J. C. Vartuli, W. J. Roth, M. E. Leonowicz, C. T. Kresge, K. D. Schmitt, C. T.-W. Chu, D. H. Olson, E. W. Sheppard, S. B. McCullen, J. B. Higgins and J. L. Schlenker, *J. Am. Chem. Soc.*, 1992, **114**, 10834.
- 5 J. S. Beck and J. C. Vartuli, *Curr. Opin. Solid State Mater. Sci.*, 1996, **1**, 76.
- 6 P. Behrens, *Angew. Chem., Int. Ed. Engl.*, 1996, **35**, 515.
- 7 S. A. Bagshaw, E. Prouzet and T. J. Pinnavaia, *Science*, 1995, **269**, 1242.
- 8 E. Prouzet and T. J. Pinnavaia, *Angew. Chem., Int. Ed. Engl.*, 1997, **36**, 516.
- 9 E. Prouzet, F. Cot, G. Nabias, A. Larbot, P. J. Kooyman and T. J. Pinnavaia, *Chem. Mater.*, 1999, **11**, 1498.
- 10 D. Zhao, J. Feng, Q. Huo, N. Melosh, G. H. Fredrickson, B. F. Chmelka and G. D. Stucky, *Science*, 1998, **279**, 548.
- 11 D. Zhao, Q. Huo, J. Feng, B. F. Chmelka and G. D. Stucky, *J. Am. Chem. Soc.*, 1998, **120**, 6024.
- 12 C. Boissière, A. Larbot, A. van der Lee, P. J. Kooyman and E. Prouzet, *Chem. Mater.*, 2000, **12**, 2902.
- 13 C. Boissière, A. Larbot and E. Prouzet, *Chem. Mater.*, 2000, **12**, 1937.
- 14 C. Boissière, A. Larbot, C. Bourgaux, E. Prouzet and C. A. Bunton, *Chem. Mater.*, 2001, **13**, 3580.
- 15 C. Boissière, M. Kümmel, M. Persin, A. Larbot and E. Prouzet, *Adv. Funct. Mater.*, 2001, **11**, 129.
- 16 J. N. Cha, G. D. Stucky, D. E. Morse and T. J. Deming, *Nature*, 2000, **403**, 289.
- 17 P. Schmidt-Winkel, P. Yang, D. I. Margolese, B. F. Chmelka and G. D. Stucky, *Adv. Mater.*, 1999, **11**, 303.
- 18 P. Schmidt-Winkel, W. W. J. Lukens, D. Zhao, P. Yang, B. F. Chmelka and G. D. Stucky, *J. Am. Chem. Soc.*, 1999, **121**, 254.
- 19 P. Tanev and T. J. Pinnavaia, *Science*, 1996, **271**, 1267.
- 20 S.-S. Kim, W. Zhang and T. J. Pinnavaia, *Science*, 1998, **282**, 1302.
- 21 G. A. Ozin, H. Yang, I. Sokolov and N. Coombs, *Adv. Mater.*, 1997, **9**, 662.
- 22 P. Behrens and G. Schechner, in *Silica 2001*, Mulhouse, France, 2001, p. 20.
- 23 S. A. Bagshaw, *Chem. Commun.*, 1999, 767.
- 24 P. Schmidt-Winkel, W. W. J. Lukens, P. Yang, D. I. Margolese, J. S. Lettow, J. Y. Ying and G. D. Stucky, *Chem. Mater.*, 2000, **12**, 686.
- 25 C. Einhorn, J. Einhorn and J.-L. Luche, *Synthesis*, 1989, 787.
- 26 C. Boissière, A. van der Lee, A. E. Mansouri, A. Larbot and E. Prouzet, *Chem. Commun.*, 1999, **20**, 2047.